



Electrospinning CoS₂/carbon nanofibers with enhanced stability as electrode materials for supercapacitors

Zhao Wang¹ · Chao Liu¹ · Gaofeng Shi¹ · Guoying Wang¹ · Qi Zhang¹ · Hongquan Zhang¹ · Ying Su¹ · Jianglei Yu¹ · Xin Li¹ · Fengfang Luo¹ · Yawen Hu¹ · Kaiqiang Yi¹

Received: 8 June 2020 / Revised: 13 July 2020 / Accepted: 27 July 2020 / Published online: 5 August 2020
© Springer-Verlag GmbH Germany, part of Springer Nature 2020

Abstract

The performance of supercapacitors is strongly influenced by the performance of electrode materials. The cobalt-sulfur compounds are used as electrode materials due to their wide range of sources, low price, and high conductivity. It was found that higher number of electron-hole pairs and higher conductivity could be provided by sulfidation. This is related to the mixing valence of Co in the cobalt sulfur compound, which promotes electron transfer to the electrolyte. During the charging and discharging process, CoS₂ is not easy to fall off from the surface of carbon nanofibers, thus increasing the doubling rate and cycling stability, due to the one-dimensional morphology of the interconnected conductive paths and excellent mechanical stability. At the current density of 1 A g⁻¹, the specific capacitance of CoS₂-CNFs reaches 488.0 F g⁻¹, over 74% of initial capacitance is retained as the current density improves from 1 to 10 A g⁻¹, and it also exhibits an excellent cycling performance with 91.0% capacitance retention after 1000 times charge/discharge cycles (at the current density of 1 A g⁻¹).

Keywords Electrospinning · CoS₂-CNFs · Supercapacitors · Electrochemical performance

Introduction

With the rapid development of economy, people's demand for energy is increasing. That has led researchers around the world to pay more attention to research on energy storage. As a novel energy storage device, supercapacitors have attracted more and more attention due to its unique advantages: short charging time, high power density, and excellent cycle stability [1, 2]. Therefore, it is expected to be used in electric vehicles, portable tools, and other fields [3]. As one of the main factors affecting the performance of supercapacitors, electrode material has many kinds [4]. As the earliest electrode material used for supercapacitors, carbon materials have advantages of wide sources, low cost, easy operation, and no toxicity [5]. Carbon material has abundant pore structure, which shows good electrochemical performance [6, 7]. As the electrode material, carbon materials have high

conductivity, stability, and high power density, and their theoretical specific capacity are insufficient, and the voltage window in the water electrolyte is narrow, resulting in low energy density, which cannot meet the needs of the current special field, thus limiting the application in supercapacitors [8, 9]. Due to their unique physicochemical properties, the transition metal compounds have several times higher specific capacity than carbon materials, and their prices are far lower than conductive polymers, showing a broad prospect in the field of preparation of tantalum capacitor electrode materials. Transition metal sulfides show a broad prospect in the field of preparation of tantalum capacitor electrode materials, because of their advantages of wide source, rich variety, low price, high conductivity, and high electrochemical activity.

Carbon nanofibers are widely used as one-dimensional carbon materials [10]. Carbon nanofibers not only have the advantages of good electrical conductivity, many chemical active sites, excellent thermal stability, high mechanical strength, and chemical resistance, but also have the advantages of large aspect ratio, compact structure, and large specific surface area, which make it an ideal electrode material [11]. But that still has the common shortcoming of all carbon materials-insufficient energy density. There are various methods for preparing carbon nanofibers.

✉ Gaofeng Shi
gaofengshi_lzh@163.com

¹ School of Petrochemical Engineering, Lanzhou University of Technology, Lanzhou city, China

Regardless of the template method, the electrochemical deposition method or the arc discharge method, there are defects such as high cost and complicated process. However, the electrospinning method has become an important method for preparing carbon nanofibers because of its simple preparation [12]. The preparation of carbon nanofibers by electrospinning requires high polymers, but high polymers are expensive. Therefore, in order to save costs, a part of the carbon materials was used to replace the polymer.

Cobalt-based sulfides in various transition metal sulfides can be used as electrode materials for supercapacitors because of their high conductivity and different stoichiometry. Cobalt-based sulfides mainly include CoS [13, 14], CoS₂ [15, 16], Co₃S₄ [17, 18], and Co₈S₉ [19, 20]. Xing [21] reported octahedron-shaped CoS₂ crystals have been successfully fabricated through a simple hydrothermal route without any surfactant or template. The as-fabricated CoS₂ electrode shows specific capacitance of 236.5 F g⁻¹ at 1 A g⁻¹. At a current density of 2 A g⁻¹, the capacity retention rate after 2000 cycles is 92.6%, which shows excellent cycle stability. Tang [22] reported a nanocomposite of cobalt disulfide (CoS₂) nanoparticles, and chemically reduced graphene oxide (RGO) sheets were prepared through a facile solvothermal method without any template. CoS₂-RGO nanocomposites have excellent specific capacitance, excellent rate performance, and good cycle stability in the voltage range -0.3 to 0.65 V. The CoS₂-RGO nanocomposite fulfilled a high capacitance of 331 F g⁻¹ at 0.5 A g⁻¹ and the capacitance retention rate was 97% after 2000 cycles.

In this work, CoS₂-CNFs composites were prepared by electrospinning and hydrothermal method. The combination of CoS₂ and carbon materials can not only make up for the shortcomings of insufficient energy density of carbon materials, but also alleviate the volume expansion of metal sulfides during charge and discharge, which can activate the synergistic effect of different materials, thereby significantly improving the electrochemical performance and cyclic stability.

Experimental

Chemicals and reagents

Cobalt acetate tetrahydrate, polyacrylonitrile, and thioacetamide were purchased from Shanghai Maclean Biochemical Technology Co., Ltd. N,N-methylformamide and acetylene black were purchased at Tianjin Tianxin Fine Chemical Development Center. Ethylene glycol, absolute ethanol, and potassium hydroxide were purchased from Tianjin Guangfu Technology Development Co., Ltd. PTFE was purchased from Guangzhou Songbai Chemical Reagent Co., Ltd. Nickel foam was purchased from Kunshan Tenehui Electronic Technology Co., Ltd.

Preparation of Co-CNFs

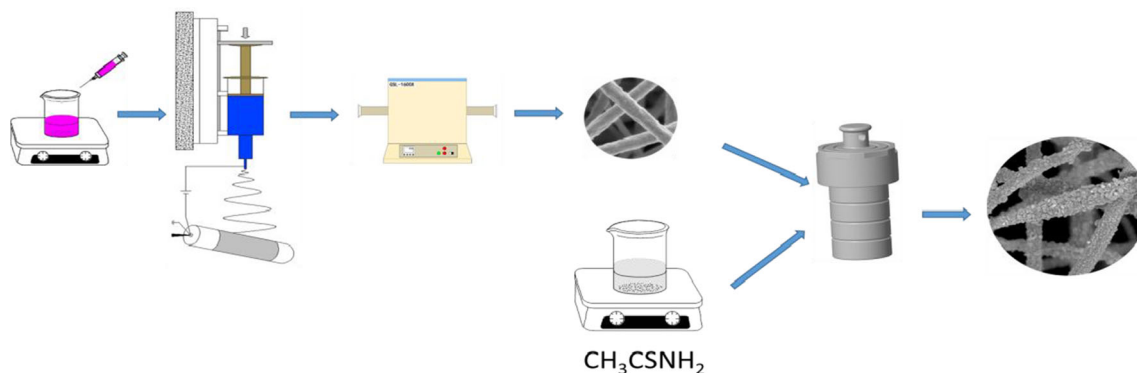
Firstly, 0.9 g polyacrylonitrile (PAN) and 0.1 g carbon materials [23] were dissolved in 10 ml n-n and dimethylformamide solution (DMF). The blend was kept under magnetic stirring for 6 h to form a viscous liquid at room temperature. Because the solubility of porous carbon in organic solvents is not ideal, the porous carbon is suspended and uniformly dispersed in the organic solution. Then, 3 mmol cobalt acetate were added into the solution with vigorous stirring at overnight. The spinning solution was sonicated for 15 min on the ultrasound machine so that it was completely uniformly mixed. A plastic syringe with a 20-gauge stainless steel needle was filled with the prepared spinning solution and then connected to the high-voltage anode. No syringe pump was used during the spinning process. A tin foil-coated cylinder served as a nanofiber collector. The distance from the tip of the needle to the collector was 20 cm. The advancing speed was 0.15 mm min⁻¹. The negative high pressure was -2 kV. The positive high pressure was 13 kV. And the room temperature was 25 °C. The nanofiber film by the above electrospinning was fixed on the magnetic boat to ensure the tension of the film. The obtained fibers were placed in a muffle furnace and pre-oxidized in air at 260 °C for 1 h, with a heating rate of 1 °C min⁻¹. Then the material was carbonized in nitrogen with a heating rate of 5 °C min⁻¹, held at 800 °C for 1 h and cooled to room temperature. Under these conditions, Co-CNFs were obtained. For performance comparison, carbon nanofibers were prepared under the same conditions without adding cobalt acetate (CNFs).

Preparation of CoS₂-CNFs

Firstly, thioacetamide at a molar ratio of 1:10 and Co-CNFs were dissolved into 60 mL of ethylene glycol and then magnetic stirring for 2 h to form homogeneous solution. Subsequently, the suspension was transferred into a 100-mL Teflon-lined stainless steel autoclave and maintained at 150 °C for 12 h in an oven, followed by natural cooling to room temperature. After cooled down, the resulting black solid product was washed with absolute ethanol and deionized water many times and dried in vacuum at 70 °C for 12 h. The entire preparation process is shown in Scheme 1.

Structure characterization

The structure of the as-prepared samples was tested by X-ray diffractometer (XRD, MSA-XD2, Rigaku, Japan) in the 2θ range of 5 to 80°. Raman spectrum was evaluated by spectrometer (JYHR800, Micro-Raman). The X-ray photoelectron spectroscopy (XPS) spectra were acquired on a scanning X-ray photoelectron spectrometer (Thermo Scientific, USA) with monochromatized Al Kα X-ray source. The surface



Scheme 1 Schematic illustration for preparation of CoS₂-CNFs

structure of the sample was observed by cold field emission type scanning electron microscope (SEM, JSM-6701F Japan Electron Optics Co., Ltd.). The microstructures of samples were imaged by transmission electron microscopy (TEM, JEOL JEM-2010).

Electrochemical characterization

The electrochemical performance measurements were carried out on a CHI660E electrochemical work station (CHI660E, Shanghai Chenhua Instrument Co., Ltd.) in 6 M KOH aqueous electrolyte with a conventional three-electrode configuration. In order to prepare a working electrode, 80 wt% active material, 15 wt% carbon black as a conductive additive, and 5 wt% polytetrafluoroethylene (PTFE) binder were mixed uniformly, using anhydrous ethanol as the solvent [24]. The paste was then loaded onto a piece of nickel foam (2.0 × 1.0 cm) with a coating area of 1 cm × 1 cm and dried at 70 °C for 12 h in a vacuum oven. Then, the electrode sheet was formed under a pressure of 5 MPa for 40 s. Cyclic voltammetry (CV), galvanostatic charge/discharge (GCD), and impedance (EIS) were performed on an electrochemical workstation using a saturated calomel electrode (SCE) and a platinum foil as a reference electrode and a counter electrode, respectively. The CV tests were conducted with a potential range of −0.2 V to 0.5 V by varying the scan rate from 5 to 30 m Vs^{−1}. The GCD tests were conducted with a potential range of −0.1 to 0.4 V at a current density from 1 to 10 A g^{−1}. Electrochemical impedance spectroscopy (EIS) tests were performed in a frequency range from 0.01 to 100,000 Hz at open circuit potential. The specific capacitance C (F g^{−1}), was calculated using the following formulae:

$$C = \frac{I\Delta t}{m\Delta V} \tag{1}$$

where *i* denotes the discharge current, Δ*t* is the discharge time, *m* is the mass load, Δ*V* is the potential window of discharge [12, 25, 26].

Results and discussion

In order to verify the crystal structure of the sample we prepared, the crystallographic structures of as-prepared CoS₂-CNFs were analyzed by X-ray powder diffraction (XRD), as shown in Fig. 1.

Compared with the standard pattern of JCPDS No. 41-1471, the CoS₂-CNFs composites, several significant diffraction peaks at 27.9°, 32.3°, 36.2°, 39.8°, 46.3°, and 54.9° are attributed to the (110), (200), (210), (211), (220), and (311) respectively [27, 28]. In addition, the diffraction peaks appeared at 22° for CoS₂-CNFs, corresponding to the (002) crystal plane of the graphite layer [29]. It can be proved that the prepared composite material contains CoS₂. Carbon nanofibers provide a support for CoS₂, which making it uniformly dispersed and preventing the imagination of CoS₂ from agglomeration.

In order to further verify whether the sample of CoS₂ and CNFs were combined or not, Raman spectroscopy tests were carried out on the CoS₂-CNFs as presented in Fig. 2. It can be seen from the figure that there is a diffraction peak around 670 cm^{−1}, which belongs to the characteristic peak of cobalt

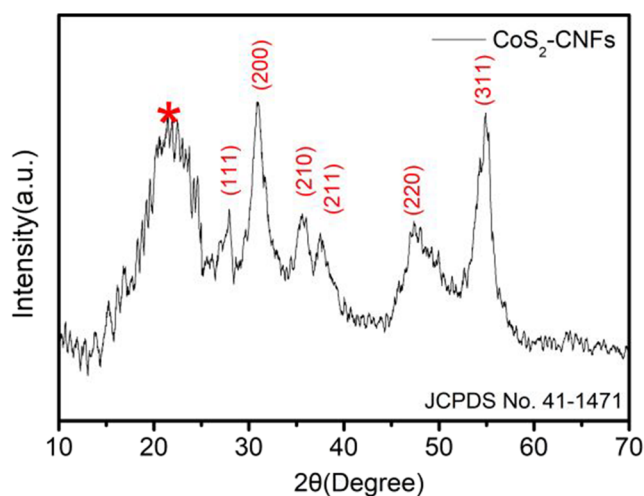


Fig. 1 XRD patterns of CoS₂-CNFs

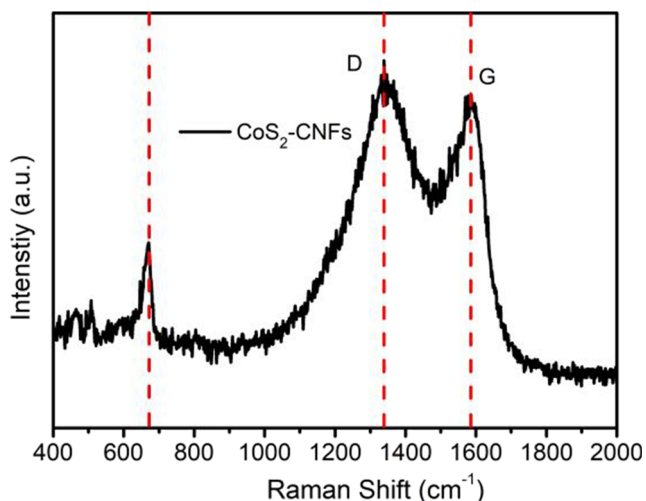


Fig. 2 Raman spectra of the CoS₂-CNFs

ions in CoS₂ [25]. At the same time, two distinct characteristic peaks were observed around 1360 cm⁻¹ and 1600 cm⁻¹, which belonged to the D peak and G peak in the carbon material, thus further illustrating the successful recombination of CoS₂ and CNFs. The D peak represents the disordered structure of the carbon material, and the G peak is the graphitized structure [30]. The intensity ratio of D band to G band (I_D/I_G) can reflect the degree of structural graphitization in the carbon materials [31]. The I_D/I_G value of the CoS₂-CNFs composite was 0.92, indicating that the carbon material in the CoS₂-CNFs composite has a higher degree of graphitization. This provides a guarantee for the excellent cycle stability of subsequent electrochemical tests.

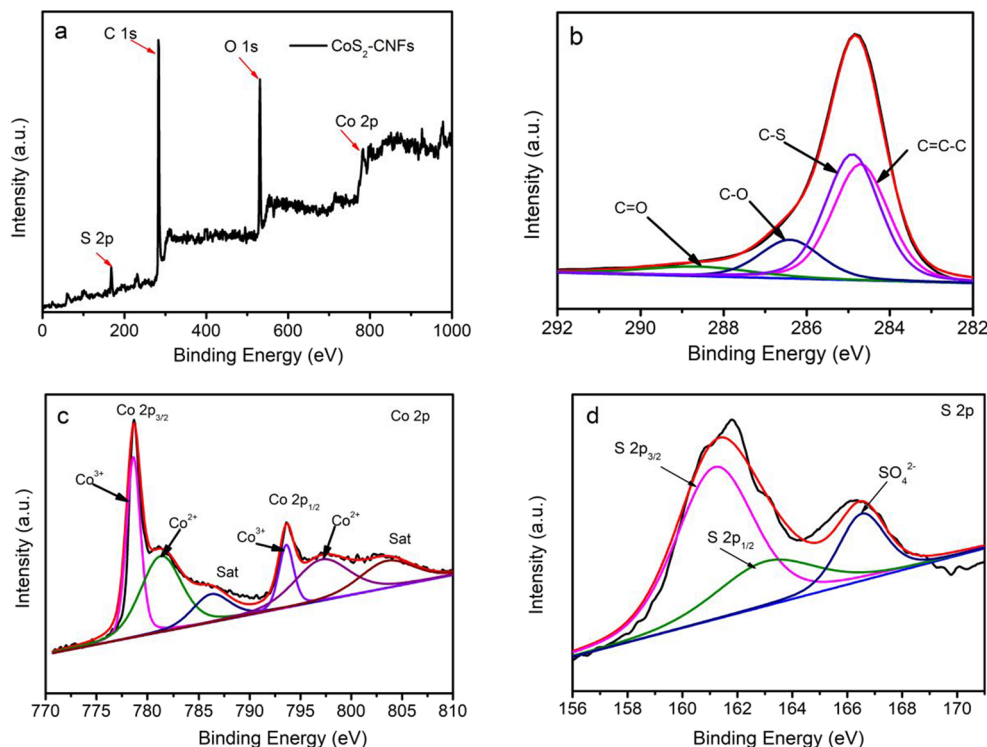
In order to further identify the phase composition of the CoS₂-CNFs composite, the binding energy and chemical states of the composite, XPS measurements were conducted, as shown in Fig. 3. Figure 3a shows the full peak spectrum of CoS₂-CNFs composite material. As can be seen from the figure, the CoS₂-CNFs composite material contains four elements C, O, Co, and S. The C element was provided by the prepared carbon material and the high polymer polyacrylonitrile (PAN) as the carbon source; the element O was introduced for preoxidation in the muff furnace in an atmosphere of air after spinning. The purpose of preoxidation in muff furnace is to enhance the toughness of carbon nanofibers; the elements Co and S were added during the experiment. Figure 3b shows the fitting peak of the C element in the composite material. There are four fitting peaks in C 1s, and the peaks about 284.7 eV, 284.9 eV, 286.4 eV, and 288.6 eV correspond to C=C-C, C-S, C-O, and C=O, respectively [12, 32]. The peak of C-S indicates that the composite contains a small amount of sulfur embedded in the carbon lattice [33]. Figure 3c shows the fitting peak of Co 2p element in the composite material. The binding energies of Co 2p_{3/2} and Co 2p_{1/2} given by Co 2p spectrum are 776.1 to 790.4 eV and 792.9 to 808.3 eV, respectively [34, 35]. The Co 2p_{1/2} peak

can also be fitted into three peaks, whose binding energy peaks appear at 793.6 eV, 796.4 eV, and 801.9 eV, respectively. The binding energy at 778 eV and 792.9 eV can be attributed to Co³⁺, and that located at 780.9 eV and 796.8 eV belongs to Co²⁺ [36, 37]. Figure 3d shows the high resolution XPS spectrum of S 2p. As can be seen that three curves can be fitted in the high-resolution XPS spectrum of S 2p, corresponding to three different types of sulfur substances. In the S 2p XPS spectrum (Fig. 3d), the curve is fitted to three peaks, which can be assigned to S in S 2p_{3/2} (161.4 eV), S 2p_{1/2} (162.5 eV), and SO⁴⁺ (167.6 eV) [38]. The existence of SO⁴⁺ may be related to the partial oxidization of sulfur species by air on the material's surface [39]. The content of each element of CoS₂-CNFs composite material is shown in Table 1. It can be seen from Table 2 that Co:S is 3.07%:6.21%, closing to 1:2, which further proves that the metal sulfide in the generated composite material exists in the form of CoS₂, that is consistent with the results of XRD analysis.

In order to study the composite of CoS₂ and carbon nanofibers from the microscopic characterization, we observed changes of the structure of the carbon fiber by SEM and TEM, as shown in Fig. 4.

Figure 4a is a scanning electron micrograph of PAN-based carbon nanofibers prepared by electrospinning. It can be seen from the figure that the PAN-based carbon nanofibers were evenly distributed, and the surface is smooth, indicating that the porous carbon prepared by doping has no effect on the structure of the carbon nanofibers. Figure 4b is a scanning electron microscope image of Co-CNFs nanofibers after carbonization. From the figure, it can be seen that fine particles were attached to the surface of the fiber and are evenly distributed on the surface of the carbon nanofibers. The introduction of metal salt ions through electrostatic spinning technology can make the cobalt ions uniformly dispersed on the fiber surface to prevent cobalt ions from agglomerating. Figure 4c is a scanning electron microscope image of CoS₂-CNFs composite material. It can be seen that the particles on the fiber of CoS₂-CNFs composite material increased significantly after hydrothermal vulcanization. That might be during the hydrothermal reaction, the sulfur ions in the thioacetamide were released and combined with the cobalt ions on the carbon nanofibers to form CoS₂, due to the high temperature. And during the sulfidation process, volume expansion broke the carbon fiber and thus appeared on the surface. As shown in Fig. 4d, that CoS₂ was evenly distributed on the surface of carbon nanofibers, rather than agglomerated together. This is because the metal salt was anchored uniformly on the carbon nanofibers by electrostatic spinning, so the metal sulfide formed during vulcanization was evenly dispersed in the carbon nanofibers. HETEM image for CoS₂-CNFs composite material (Fig. 4e) reveals a lattice spacing of 0.248 nm, which corresponds to the (210) plane. Figure 4f is the SAED

Fig. 3 XPS of CoS₂-CNFs. **a** Full spectrum. **b** C 1 s energy spectrum. **c** Co 2p energy spectrum. **d** S 2p energy spectrum



diffraction ring diagram of CoS₂-CNFs composite material, from which the (111), (200), (210), (220), and (311) crystal planes of CoS₂ can be detected, proving that the CoS₂ particles are anchored on the surface of CNF. The crystalline nature is consistent with the XRD results. The element mapping shown in Fig. 4g demonstrates a uniform distribution of Co, S, C, and O elements on the surface of the CoS₂-CNFs composite material. All the tests above indicated that CoS₂ and CNFs were successful.

Electrochemical property testing was an important method to characterize electrode materials. We applied the electrochemical workstation to test the electrochemical properties of the composite material CNFs, Co-CNFs, and CoS₂-CNFs, as shown in Fig. 5. Figure 5a shows the cyclic volt-amperes of CNFs, Co-CNFs, and CoS₂-CNFs composites at 20 mV S⁻¹. It can be seen from the figure that Co-CNFs and CoS₂-CNFs had a pair of redox peaks, and the CV curve area of CoS₂-CNFs was the largest, and the electrochemical performance was the best. However, because the electrochemical range was not suitable, CNFs showed a rectangular shape that was not an electric double layer. Figure 5b shows the GCD of CNFs, Co-CNFs, and CoS₂-CNFs composites. Under the current density

of 1 A g⁻¹, the specific capacitance of CNFs, Co-CNFs, and CoS₂-CNFs composites were 15 F g⁻¹, 358.8 F g⁻¹, and 488 F g⁻¹. The CoS₂-CNFs composite has the longest discharge time and the best electrochemical performance. In addition, there is a platform for the Co-CNFs and CoS₂-CNFs composites during charging and discharging, namely, there is a pair of redox peaks, which is consistent with the cyclic volt-ampere curve. Figure 5c shows the variation of specific capacitance with the increase of current density. At the current density of 10 A g⁻¹, the specific capacitance of CNFs, Co-CNFs, and CoS₂-CNFs composites were 4 F g⁻¹, 248 F g⁻¹, and 360 F g⁻¹. When the current density increased by 10 times, the capacitance retention rates of CNFs, Co-CNFs, and CoS₂-CNFs composites were 22%, 69.1%, and 74% respectively. The CoS₂-CNFs composites have good rate performance. As the current density increases in supercapacitors, it is a common phenomenon that the specific capacitance decreases. That is because during constant current charging and discharging, due to insufficient contact between the electrode material and the electrolyte at high current density, which leads to the redox reaction, is insufficient. Ion and electron

Table 1 Surface element content of CoS₂-CNFs

Sample	C %	O %	Co %	S%
CoS ₂ -CNFs	79.07	11.65	3.07	6.21

Table 2 Specific capacitance of CoS₂-CNFs (F g⁻¹)

Sample	C (F/g) 1 A/g	C (F/g) 2 A/g	C (F/g) 4 A/g	C (F/g) 6 A/g	C (F/g) 8 A/g	C (F/g) 10 A/g
CoS ₂ -CNFs	488.0	442.4	421.8	396.4	378.0	360.0

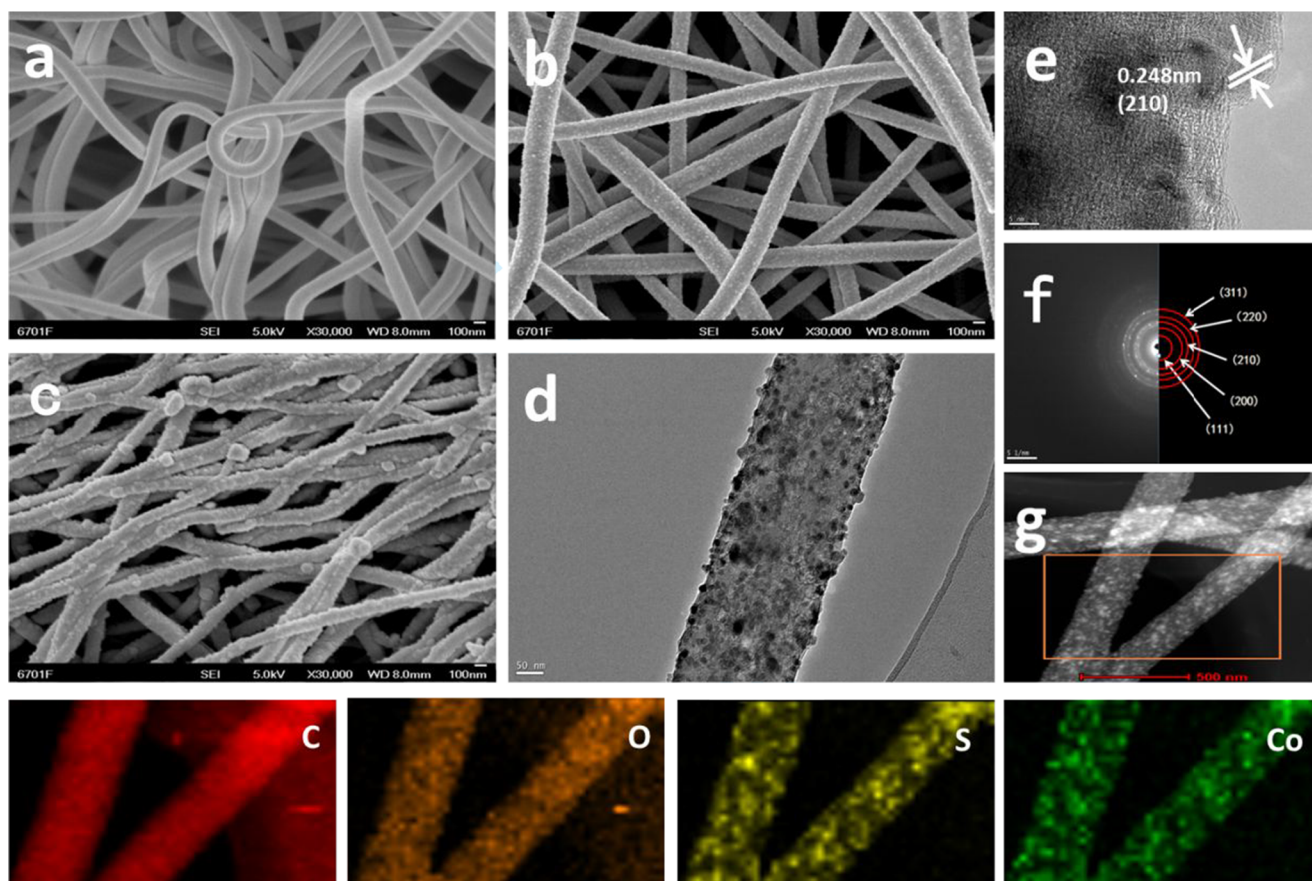
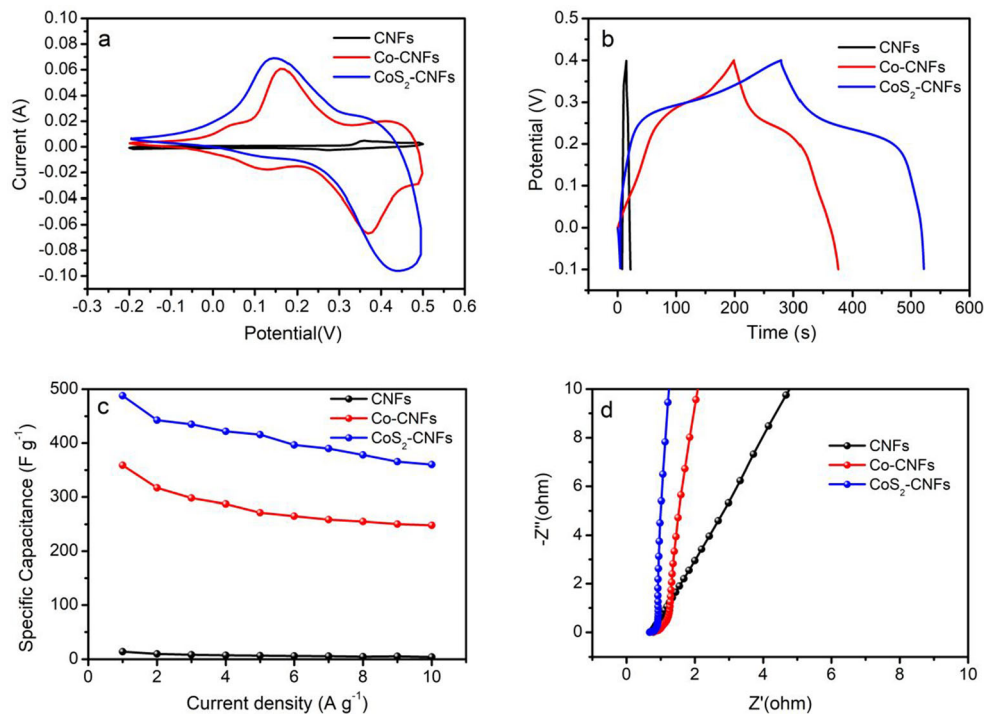


Fig. 4 **a** SEM image of PAN-based carbon nanofibers. **b** SEM image of Co-CNFs composite material. **c** SEM image of CoS₂-CNFs composite material. **d** TEM image of CoS₂-CNFs composite material. **e** HRTEM

image of CoS₂-CNFs composite. **f** SAED diffraction ring diagram of CoS₂-CNFs composite. **g** The TEM EDS elemental mapping of Co, S, C, and O, for the CoS₂-CNFs

Fig. 5 Electrochemical performance of CNFs, Co-CNFs and CoS₂-CNFs. **a** CV curves for CNFs, Co-CNFs and CoS₂-CNFs at a scan rate of 20 mV s⁻¹. **b** GCD curves of all the samples at the current density of 1 A g⁻¹. **c** Specific capacitance of CNFs, Co-CNFs, and CoS₂-CNFs versus various current densities from 1 to 10 A g⁻¹. **d** Electrochemical impedance spectra (EIS) of the CNFs, Co-CNFs, and CoS₂-CNFs



transport is difficult during fast charge and discharge, and cannot be carried out sufficiently, so that the chemical valence state of metal cobalt ions is not fully converted in the electrolyte. Figure 5d is the AC impedance diagram of the composite material. The AC impedance diagram includes a straight line with a semicircle in the high-frequency region and a slope in the low-frequency region. The intercept on the X axis is usually used to represent the solution resistance, R_s , which consists of the internal resistance of the electrode material and the contact resistance at the electrode/electrolyte interface [40, 41]. The lower the R_s value, the more sufficient the contact between the electrode material and KOH in the electrolyte, and the smaller the contact resistance between the resistor and the interface between the two, which is conducive to the electrolyte reaching the surface of the electrode more effectively, resulting in good activation effect, complete redox reaction, and complete chemical valence conversion of cobalt element in the electrolyte. In the low-frequency region, the slope of the inclined line is related to the Warburg resistance (W), which reflects the diffusion rate of ions from the electrolyte to the electrode material surface. The closer the slope of the line is to 90° , the faster the diffusion rate of ions to the electrode surface [42]. Based on the above electrochemical analysis, the CoS_2 -CNFs composite has the best electrochemical performance.

The electrochemical test of CoS_2 -CNFs composite was performed below, as shown in Fig. 6. Figure 6a shows the CV curve of CoS_2 -CNFs at different scanning rates from 5 to 30 mV s^{-1} in the potential window from -0.2 to 0.5 V . It can be seen from the figure that there is a pair of redox peaks at different scanning speeds, instead of the ideal rectangular double electric layer, indicating that the CoS_2 -CNFs composite material as the electrode of supercapacitor is not simply electrostatic charge adsorption and ion diffusion, but shows the electrochemical performance of pseudocapacitance. As can be seen from the figure, at a sweep rate of 5 mV^{-1} , there was a pair of significant redox peaks. As the scanning speed increases, especially at a scanning speed of 30 mV s^{-1} , polarization occurs, and the cyclic voltammetry curve was deformed, possibly due to the presence of ohmic voltage drop and dispersion capacitance at large scanning speeds. In addition, it can be seen from the figure that the position of the redox peak was shifted. That is because the redox reaction cannot satisfy the electron neutralization, which limits the diffusion rate of ions. At present, the electrochemical reaction mechanism of metal sulfide in the alkaline electrolyte is not particularly clear, but the element sulfur and oxygen belong to the same race. So referring to the Faraday reaction of metal oxide in the alkaline electrolyte, the following is the possible storage mechanism of CoS_2 -CNFs composite material as the

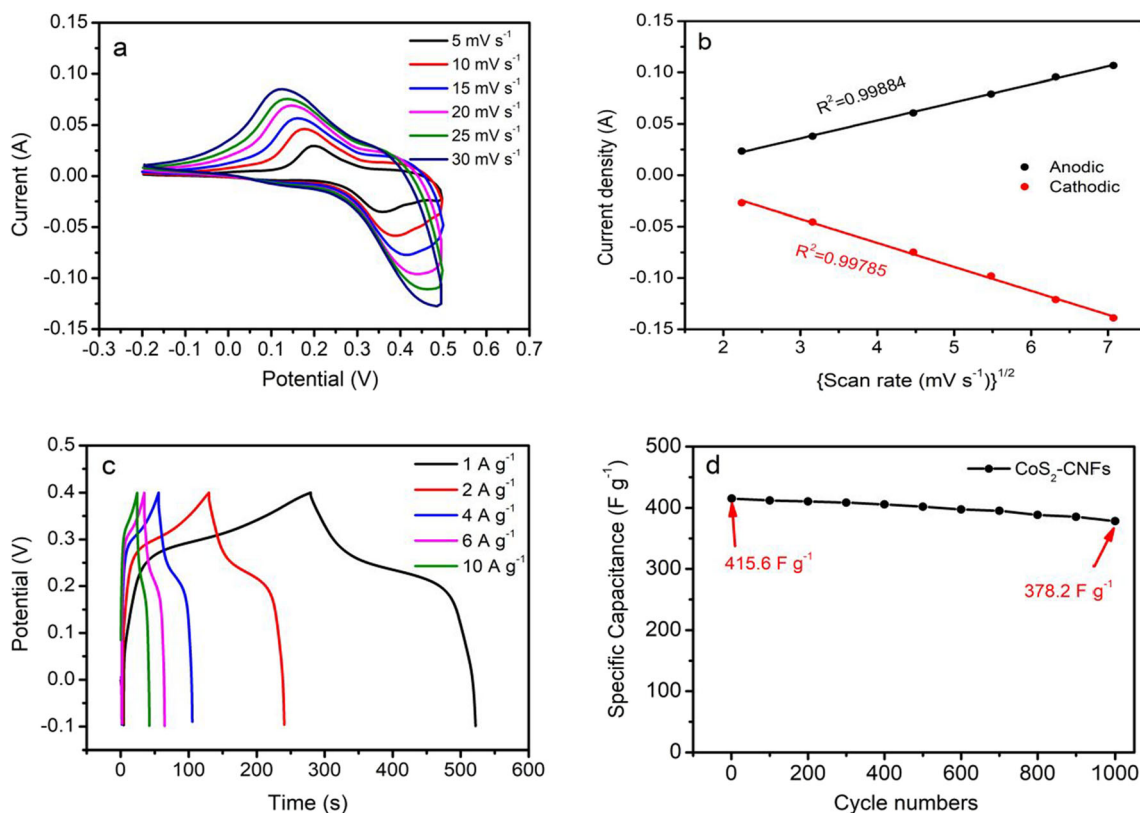
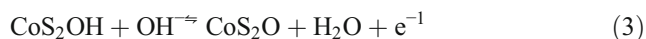
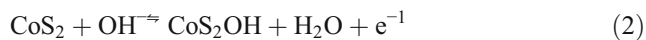


Fig. 6 Electrochemical performance of CoS_2 -CNFs. **a** CV curves at scan rates ranging from 5 to 30 mV s^{-1} . **b** GCD curves of at different current densities from 1 to 10 A g^{-1} . **c** The relationship between the main redox

peak current and the square root of scan rate for the two electrodes. **d** CoS_2 -CNFs in specific capacitance retention rates at the current density of 5 A g^{-1} after 1000 cycle

electrode material in alkaline solution [43]:



As can be seen from the figure, with the increase of scanning speed, both the intensity and position of the redox peak increase. The output position of oxidation peak moves in the negative direction, while the reduction peak moves in the positive direction. That is because when the redox reaction occurs, the diffusion resistance increases, limiting the diffusion speed. So it cannot quickly neutralize the electrons generated during the redox reaction. Figure 6b shows the relationship between the peak current (anode and cathode) and the square root of the scanning rate. By increasing the scanning rate, we can see the change in the position of the redox peak of the CoS₂-CNFs composite, which may be due to the more complete redox reaction occurred during the reaction. It can be seen from the figure that the peak current shows a linear change. The correlation coefficient (R^2) has a high phase relationship of 0.99884 anode peak and 0.99785 cathode peak. So the surface peak is linearly related to the square root of the scanning rate, which can be explained by the classic Sevcik equation [44]:

$$I_p = 2.69 \times 10^5 n^{3/2} A D_0^{1/2} V^{1/2} C_0 \quad (4)$$

where I_p is the peak current density, N is the electron transfer number, A is the contact surface area of the electrode, D_0 is the diffusion coefficient of the rate limiting species such as proton, V is the scanning rate, and C_0 is the proton concentration.

It can be seen from the above formula that, as long as the reaction type is determined, the square root of peak current density and scanning speed is linear when other variables are fixed, indicating that the redox mechanism is limited by surface reaction. Figure 6c shows the constant current charge-discharge diagram of CoS₂-CNFs composite material under different current densities. It can be seen from the figure that there is a platform in charge and discharge, which is not an isoscele-like triangle with double electrical layers, consistent with the redox peak in the CV curve. Therefore, the energy storage and release of CoS₂-CNFs composite material is characterized by redox reaction. The charging and discharging time decreases with the increase of current density. Table 1 shows the specific capacitance of CoS₂-CNFs composite material at different current densities. Therefore, the above electrochemical performance analysis shows that the CoS₂-CNFs composite material as the electrode material of the supercapacitor is the energy storage characteristic of the pseudocapacitor. Figure 6d shows the CoS₂-CNFs cycle characteristics at a current density of 5 A g⁻¹ with 1000 cycles of charge and discharge. The CoS₂-CNFs capacitance retention rate was 91.0% after 1000 cycles.

Table 3 The electrochemical data of CoS₂ as electrode material

Cobalt material	Current density	Specific capacitance	References
CoS ₂ /NCNTF	1.0 A g ⁻¹	937.0 m Ah g ⁻¹	[15]
CoS ₂	1.0 A g ⁻¹	236.5 F g ⁻¹	[21]
CoS ₂ -RGO	0.5 A g ⁻¹	331 F g ⁻¹	[22]
CoS ₂ -CNFs	1.0 A g ⁻¹	488.0 F g ⁻¹	This work

To evaluate the superiority of the prepared electrode materials, Table 3 lists our results compared to previously published of CoS₂ as electrode material.

Conclusions

In summary, we had developed a self-standing CoS₂-CNFs electrode with CoS₂ nanoparticles either encapsulated in or attached to the interconnected one-dimensional carbon fibers. Cobalt metal ions are added to carbon nanofibers through electrostatic spinning, so there is less chance for CoS₂ to fall off carbon nanofibers, and the synergistic effect of the two is better played. Although the conductivity of cobalt dioxide is high, volume expansion occurs, reducing the contact area with the electrolyte. And there was a serious volume change and dissolution of polysulfide compounds accompanying the CoS₂ conversion reaction. Carbon nanofibers can reduce the volume change during charge and discharge and increase the proportion of active substances involved in the reaction. Carbon nanostructured surface morphology provides more ion intercalation or deintercalation at the electrochemically active sites that can enhance performance during electrochemical reactions. The CoS₂-CNFs exhibited excellent performance with a high specific capacitance of 488 F g⁻¹ at a current density of 1 A g⁻¹. After charging and discharging for 1000 cycles at a current density of 5 A g⁻¹, the capacitance retention value was maintained at 91.0%. The remarkable electrochemical properties of CoS₂-CNFs had indicated that it was a promising electrode material for supercapacitors.

Funding information This work was supported by the National Natural Science Foundation of China (21567015), the National Key Research and Development Program of China (2016YFC0202900), Lanzhou University of Technology Hongliu First-class Discipline Construction Program (Support), and Lanzhou University of Technology Hongliu Science Fund for Young Scholars (2018 Support).

References

- Dunn B, Kamath H, Tarascon JM (2011) Electrical energy storage for the grid: a battery of choices. *Science* 334(6058):928–935
- Zhang HB, Nai JW, Yu L, Lou XW (2017) Metal-organic-framework-based materials as platforms for renewable energy and environmental applications. *Joule* 1(1):77–107

3. Zhang ZS, Zhang YF, Yang K, Yi KY, Zhou ZH, Huang AP, Mai KC, Lu XH (2015) Three-dimensional carbon nanotube ethylvinylacetate polyaniline as a high performance electrode for supercapacitors. *J Mater Chem A* 3(5):1884–1889
4. Chen H, Guo YC, Wang F, Wang G, Qi PR, Guo XH, Dai B, Yu F (2017) An activated carbon derived from tobacco waste for use as a supercapacitor electrode material. *New Carbon Mater* 32(6):592–599
5. Han Y, Lai ZZ, Wang ZF, Yu MH, Tong YX, Lu XH (2018) Designing carbon based supercapacitors with high energy density: a summary of recent progress. *Chem-Eur J* 24(29):7312–7329
6. Teng ZC, Han KH, Li JX, Gao Y, Li M, Ji TT (2020) Ultrasonic-assisted preparation and characterization of hierarchical porous carbon derived from garlic peel for high-performance supercapacitors. *Ultrason Sonochem* 60:104756–104765
7. Fan L, Yang L, Ni XY, Han J, Guo R, Zhang CF (2016) Nitrogen-enriched meso-macroporous carbon fiber network as a binder-free flexible electrode for supercapacitors. *Carbon* 107:629–637
8. Choi C, Lee JA, Choi AY, Kim YT, Lepro X, Lima MD, Baughman RH, Kim SJ (2014) Flexible supercapacitor made of carbon nanotube yarn with internal pores. *Adv Mater* 26(13):2059–2065
9. Borenstein A, Hanna O, Ran A, Luski S, Brousse T, Aurbach D (2017) Carbon-based composite materials for supercapacitor electrodes: a review. *J Mater Chem A* 5:12653–12672
10. Kim C, Yang KS (2003) Electrochemical properties of carbon nanofiber web as an electrode for supercapacitor prepared by electrospinning. *Appl Phys Lett* 83(6):1216–1218
11. Zhao H, Wang L, Jia D, Xia W, Li J, Guo ZP (2014) Coal based activated carbon nanofibers prepared by electrospinning. *J Mater Chem A* 2(24):9338–9344
12. Wang Z, Liu C, Shi GF, Ma H, Jiang X, Zhang Q, Zhang HQ, Su Y, Yu JL, Jia SM (2019) Preparation and electrochemical properties of CoS₂/carbon nanofiber composites. *Ionics* 25(10):5035–5043
13. Justin P, Rao GR (2010) CoS spheres for high-rate electrochemical capacitive energy storage application. *Int J Hydrog Energy* 35(18):9709–9715
14. Hu H, Guan BY, Lou XW (2016) Construction of complex CoS hollow structures with enhanced electrochemical properties for hybrid supercapacitors. *Chem* 1(1):102–113
15. Zhang JT, Yu L, Lou XW (2017) Embedding CoS₂ nanoparticles in N-doped carbon nanotube hollow frameworks for enhanced lithium storage properties. *Nano Res* 10:4298–4304
16. Zhang YH, Wang NN, Sun CH, Lu ZX, Xue P, Tang B, Bai ZC, Dou SX (2018) 3D spongy CoS₂ nanoparticles/carbon composite as high-performance anode material for lithium/sodium ion batteries. *Chem Eng J* 332:370–376
17. Zhang QF, Xu CM, Lu BA (2014) Super-long life supercapacitors based on the construction of Ni foam/graphene/Co₃S₄ composite film hybrid electrodes. *Electrochim Acta* 132:180–185
18. Wang QH, Jiao LF, Du HM, Si YC, Wang YJ, Yuan HT (2012) Co₃S₄ hollow nanospheres grown on graphene as advanced electrode materials for supercapacitors. *J Mater Chem* 22(40):21387–21391
19. Kumar N, Raman N, Sundaresan A (2014) Synthesis and properties of cobalt sulfide phases: CoS₂ and Co₉S₈. *Z Anorg Chem* 640(6):1069–1074
20. Zhang YH, Wang NN, Xue P, Liu YL, Tang B, Bai ZC, Dou SX (2018) Co₉S₈@carbon nanospheres as high-performance anodes for sodium ion battery. *Chem Eng J* 332(2018):370–37623
21. Xing JC, Zhu YL, Zhou QW, Zheng XD, Jiao QJ (2014) Fabrication and shape evolution of CoS₂ octahedrons for application in supercapacitors. *Electrochim Acta* 136:550–556
22. Tang JH, Shen JF, Li N, Ye MX (2014) A free template strategy for the synthesis of CoS₂-reduced graphene oxide nanocomposite with enhanced electrode performance for supercapacitors. *Ceram Int* 40(10):15411–15419
23. Shi GF, Wang Z, Liu C, Wang GY, Jia SM, Jiang X, Dong YC, Zhang Q, Zhang HQ, Li X, Luo FF (2019) Preparation and electrochemical performance of porous carbon from Fujimoto bean. *Int J Electrochem Sci* 14:5259–5270
24. Luo FL, Li J, Yuan HY, Xiao D (2014) Rapid synthesis of three-dimensional flower-like cobalt sulfide hierarchitectures by microwave assisted heating method for high-performance supercapacitors. *Electrochim Acta* 123:183–189
25. Xie J, Liu SY, Cao GS, Zhu TJ, Zhao XB (2013) Self-assembly of CoS₂/graphene nanoarchitecture by a facile one-pot route and its improved electrochemical Li-storage properties. *Nano Energy* 2(1):49–56
26. Vinodh R, Gopi CM, Yang ZM, Deviprasath C, Atchudan R, Raman V, Yi M, Kim HJ (2020) Novel electrode material derived from porous polymeric organic framework of phloroglucinol and terephthaldehyde for symmetric supercapacitors. *J Energy Storage* 28:101283–101293
27. Yi JN, Qing Y, Wu CT, Zeng YX, Wu YQ, Lu XH, Tong YX (2017) Lignocellulose-derived porous phosphorus-doped carbon as advanced electrode for supercapacitors. *J Power Sources* 351:130–137
28. Zhang JT, Li Z, Lou XW (2017) A freestanding selenium disulfide cathode based on cobalt disulfide-decorated multichannel carbon fibers with enhanced lithium storage performance. *Angew Chem Int Ed* 56(45):14107–14112
29. Zhang L, Zhang F, Yang X, Leng K, Huang Y, Chen YS (2013) High-performance supercapacitor electrode materials prepared from various pollens. *9(8):1342–1347*
30. Hao XD, Wang J, Ding B, Wang Y, Chang Z, Dou H, Zhang XG (2017) Bacterial-cellulose-derived interconnected meso-microporous carbon nanofiber networks as binder-free electrodes for high-performance supercapacitors. *J Power Sources* 352:34–41
31. Jung HC, Vinodh R, Gopi CM, Yi M, Kim HJ (2019) Novel composite electrode material derived from hypercross-linked polymer of pyrene and polyaniline for symmetric supercapacitor. *Mater Letters* 257:126732–126737
32. Vinodh R, Babu RS, Gopi CM, Deviprasath C, Atchudan R, Samyn LM, Barros ALF, Kim HJ, Yi M (2020) Influence of annealing temperature in nitrogen doped porous carbon balls derived from hypercross-linked polymer of anthracene for supercapacitor applications. *J Energy Storage* 28:101196–101207
33. Faber MS, Dziedzic R, Lukowski R, Kaiser NS, Ding Q, Jin S (2014) High-performance electrocatalysis using metallic cobalt pyrite (CoS₂) micro- and nanostructures. *J Am Chem Soc* 136(28):10053–10061
34. Zeng PY, Li JW, Ye M, Zhuo KF, Fang Z (2017) In situ formation of Co₉S₈/N-C hollow nanospheres by pyrolysis and sulfurization of ZIF-67 for high-performance lithium-ion batteries. *Chem Eur J* 23(40):9517–9524
35. Chul HD, Vinodh R, Gopi CM, Deviprasath C, Kim HJ, Yi M (2019) Effect of cobalt and zinc ratio on the preparation of zeolitic imidazole framework (ZIF): synthesis, characterization and supercapacitor application. *Dalton Trans* 48:14808–14819
36. Zhang X, Liu RR, Zang YP, Liu GQ, Wang GZ, Zhang YX, Zhang HM, Zhao HJ (2016) Co/CoO nanoparticles immobilized on Co-N-doped carbon as trifunctional electrocatalysts for oxygen reduction, oxygen evolution and hydrogen evolution reactions. *Chem Commun* 35(52):5946–5949
37. Feng LL, Fan MH, Wu YY, Liu YP, Li GD, Chen H, Chen W, Wang DJ, Zou XX (2016) Metallic Co₉S₈ nanosheets grown on carbon cloth as efficient binder-free electrocatalysts for the hydrogen evolution reaction in neutral media. *J Mater Chem A* 4(18):6860–6867

38. Dou S, Tao L, Huo J, Wang SY, Dai LM (2016) Etched and doped Co₉S₈/graphene hybrid for oxygen electrocatalysis. *Energy Environ Sci* 4(9):1320–1326
39. Gao XC, Zheng XJ, Tian JH, Jin C, Ke K, Yang RZ (2016) Cobalt sulfide embedded in porous nitrogen-doped carbon as a bifunctional electrocatalyst for oxygen reduction and evolution reactions. *Electrochim Acta* 191:776–783
40. Xiao Z, Xiao GZ, Shi MH, Zhu Y (2018) Homogeneously dispersed Co₉S₈ anchored on nitrogen and sulfur co-doped carbon derived from soybean as bifunctional oxygen electrocatalysts and supercapacitor. *ACS Appl Mater Interfaces* 19(10):16436–16448
41. Justin AS, Vickraman P, Reddy BJ (2019) Carbon sphere@nickel sulfide core-shell nanocomposite for high performance supercapacitor application. *Curr Appl Phys* 3(19):295–302
42. Chen C, Wu MK, Tao K, Zhou JJ, Li YL, Han X, Han L (2018) Formation of bimetallic metal-organic framework nanosheets and their derived porous nickel-cobalt sulfides for supercapacitors. *Dalton Trans* 47(16):5639–5645
43. Mao ML, Mei L, Wu LC, Li QH (2014) Facile synthesis of cobalt sulfide/carbon nanotube shell/core composites for high performance supercapacitors. *RSC Adv* 4(23):12050–12056
44. Liu B, Yuan HT, Zhang YS, Zhou ZX, Song DY (1999) Cyclic voltammetric studies of stabilized α -nickel hydroxide electrode. *J Power Sources* 79(2):277–280

Publisher's note Springer Nature remains neutral with regard to jurisdictional claims in published maps and institutional affiliations.